

RESEARCH

Open Access



Relationships between land use types and urban heat island intensity in Hulu Langat district, Selangor, Malaysia

Muhammad Rendana¹, Wan Mohd Razi Idris², Sahibin Abdul Rahim³, Hazem Ghassan Abdo^{4*} , Hussein Almohamad⁵, Ahmed Abdullah Al Dughairi⁵ and Motrih Al-Mutiry⁶

Abstract

Background Urban heat island (UHI) is an urban climate phenomenon that primarily responds to urban conditions and land use change. The extent of hard surfaces significantly influences the thermal properties of the land. To address this issue, a novel approach quantifying the association between land use and UHI is developed. This study offers a new technique for effectively estimating the effect of land use on the UHI intensity using the combination of urban heat intensity index (UHII) and land contribution index (LCI) derived from Landsat 8 OLI images. The time-series thermal effect of land use on the UHI intensity can be determined according to the ratio in mean temperature between specific land use and the whole study site. The study was conducted in the Hulu Langat district, Malaysia during 2014–2021.

Results The UHI intensity rose from 0.19 in 2014 to 0.70 in 2021. The negative value of LCI for vegetation areas and water bodies obtained its negative contribution to the urban heat island, while the positive value of LCI for bare areas and built-up areas showed its positive effect on the urban heat island. The LCI value for urban areas showed a significant increase in the 7 years such as 0.51, 0.66, 0.69, and 0.75 for periods 2014, 2016, 2018, and 2021, respectively. The change in LCI from 2014 to 2021 for the transformation of bare area and forest was recorded to be 0.23 and – 0.02, respectively. Thus, the conversion of forests into urban areas had a negative effect on the increment of UHI intensity.

Conclusions Overall, these findings are useful for policy-making agency in developing an effective policy for reducing high UHI intensity and planning long-term land use management.

Keywords Geospatial technology, Urban heat island, Land contribution index, Land surface temperature, Environment

*Correspondence:

Hazem Ghassan Abdo
hazemabdo@tartous-univ.edu.sy

Full list of author information is available at the end of the article



© The Author(s) 2023. **Open Access** This article is licensed under a Creative Commons Attribution 4.0 International License, which permits use, sharing, adaptation, distribution and reproduction in any medium or format, as long as you give appropriate credit to the original author(s) and the source, provide a link to the Creative Commons licence, and indicate if changes were made. The images or other third party material in this article are included in the article's Creative Commons licence, unless indicated otherwise in a credit line to the material. If material is not included in the article's Creative Commons licence and your intended use is not permitted by statutory regulation or exceeds the permitted use, you will need to obtain permission directly from the copyright holder. To view a copy of this licence, visit <http://creativecommons.org/licenses/by/4.0/>.

Background

In this decade, urbanization and migration have been the most influential anthropogenic activities (Zhou et al. 2019; Roy et al. 2022). The rapid increase in population and people's movement from green areas to crowded areas result in urban and suburban environmental instability (Wang et al. 2020; Rendana et al. 2022; Correia Filho et al. 2023). Several studies have reported urbanization process will alter the energy and water cycle and influence air diffusion (Cai et al. 2019; Wei et al. 2021; Karuppasamy et al. 2022). Thus, studying the urban climate and other related factors is necessary to learn more about consequences of urbanization. The difference in surface temperature between urban and rural areas is commonly referred to as the urban heat island (UHI). This occurrence coincides with the expansion of urbanization as a result of changes in urban thermal characteristics, which increase the surface temperature in urban land.

Currently, with the advantage of extensive spatial coverage and temporal data, the remote sensing technique using satellites can be used in various studies including UHI effect (Lyu et al. 2022; Nasir et al. 2022; Rendana et al. 2021a). Several satellites such as Landsat, MERIS, ASTER, and MODIS data were all effective for UHI studies in different areas (Fabrizi et al. 2010; Shirani-Bidabadi et al. 2019; Wang et al. 2019; Deng et al. 2022). However, because of its large temporal characteristic and medium pixel resolution, Landsat 8 data are frequently chosen by many studies (Wang et al. 2019; Rendana et al. 2021b). For instance, Tepanosyan et al. (2021) assessed spatial variation of UHI intensity in Yerevan, Armenia using Landsat 5 TM and Landsat 7 ETM+ data. The UHI intensity in Worcester, MA, USA was also investigated using the Landsat 8 TIRS data by Elmes et al. (2020).

Investigations of UHI effect have been widely carried out in recent years (Cheela et al. 2021). A previous study by Rahaman et al. (2022) revealed a strong positive relationship between carbon emission and land surface temperature (LST) and carbon emission and UHI ($R^2 > 0.79$, $p < 0.001$), indicating that carbon emission made a high contribution to the LST rise and UHI effect. Another study in Kuwait by AlDousari et al. (2022) has found the conversion of 27% bare area and 5% vegetative land into built-up area could increase LST by 5 °C and UHI intensity by 0.86. Kafy et al. (2022) found a rapid development of built-up lands in Sylhet City, Bangladesh would result in stronger UHI effect. AlDousari et al. (2023) used the Landsat image and cellular automata and artificial neural network models to predict future thermal comfort zone in Kuwait. Their study highlighted during the future scenario, there was an increase in urban lands and a very high

thermal comfort zone was majorly distributed in urban and bare areas. Saha et al. (2022) revealed that urban development raised LST by 7 °C in summer and 6 °C in winter periods. Kafy et al. (2021) found a mean 4 °C higher LST was observed in urban land as compared to vegetation areas. Another study assumed that if the urban expansion continuously occurred, the study area would sustain a temperature above 38 °C in the predicted scenario (Kafy et al. 2020). In China, Zhang et al. (2023) applied the artificial neural network-cellular automata and IWOA–LSTM models to estimate the alteration of LST and land use change. They found the area with high temperatures (> 30 °C) was developing in the urban area, whereas the vegetation and water areas with low temperatures slowly.

Furthermore, the relationship between land use type and the UHI effect has recently been thoroughly investigated. The alteration of land uses is an important driver of intensive migration and urbanization, resulting in the change of landscape properties and also influencing the conversion of energies from the surface to the atmosphere (Nimish et al. 2020). Various land use categories have different effects on thermal conditions in urban areas. The conversion of land use from rural to urban areas influences temperature patterns which are similar to the global warming phenomenon (Dhar et al. 2019; Taiwo et al. 2023). Several previous studies have reported land use in urban areas and its associated thermal effect has unusually distinct attributes (Huang et al. 2019). Nurwanda and Honjo (2020) have applied urban land use expansion and the increment of the population to assess land thermal trends in Bogor, Indonesia. In addition, the link between LST and land use type has been evaluated in India (Mukherjee and Singh 2020). Therefore, it can be assumed that land use change is not the only factor affecting the UHI, and other human activities can also contribute to it.

Based on the above studies, the impacts of bare area and built-up area on UHI intensity have been extensively discussed. Urbanization is a result of changing bare area or vegetation to built-up area, thus it is prominent to analyze the contribution of built-up area to UHI intensity. The urban heat intensity index (UHII) was applied in this current study that allows the character of urban LST making it useful to evaluate the UHI intensity in low, medium, and large-sized cities with altering native land use around the area. Therefore, this study aims to assess the UHI intensity from 2014 to 2021 in Hulu Langat district of Malaysia using the UHII from Landsat 8 satellite data. Furthermore, the effect of each land use on change of LST was analyzed using the land contribution index (LCI) for years 2014, 2016, 2018 and 2021 to assess the divergence in the impact of each land use on the LST

with the alteration of land use change and urbanization factor.

Materials and methods

Study area

Hulu Langat is one of the most populous districts in Selangor State, Malaysia (101°44′0″E–101°52′0″E, 2°56′0″N–3°12′0″N) (Fig. 1). It is located in the south-east part of Selangor, where it has a mix of rural and urban settlements, with a predominant population living in cities nearby the capital city, Kuala Lumpur. Hulu Langat is a metro and educational city, because it has various public transport and famous universities, which makes migration activities easier and more intense. The total area of Hulu Langat was around 829.44 km², with seven main districts. The population of Hulu Langat was 1,400,461 people in 2020. The region had a tropical rain-forest climate (classification: Af, based on Koppen's classification) with two monsoons: the northeast monsoon (November–March) and the southwest monsoon (May–September). The annual high temperature is 32 °C and the mean annual precipitation is 2067 mm. Hulu Langat's urbanization degree ranked top ten in the country as a developed urban city, which led to the UHI effect and poor air quality. This decade has occurred a significant increase in urban area expansion, contributing to high temperatures in urban areas.

Data sources

To assess land surface temperature and estimate UHI intensity over the Hulu Langat district, the Landsat 8 data (OLI product type 1:30 m resolution) from 2014 to 2021 were obtained in the same month of July (during the peak of the dry season) for analyzing the UHI intensity variation and land use classification (Table 1). Landsat 8 data were acquired from the USGS Earth Explorer website. Then, the Landsat 8 TIRS images (30 m resolution) were used to analyze the land surface temperature over the study area in the same period. In addition, a land use map that was produced by the Department of Agriculture was used to ascertain the estimated land use map in this study. Other data, like the boundary of the Hulu Langat region, roads, and rivers were obtained from Google Earth.

Land use classification and land surface temperature

The processing software for satellite data, raster data, and vector data was carried out using ArcGIS Ver. 10. First, all satellite images and vector data were projected to the Kertau RSO Malaya meter coordinate system. The border of the study area was then used to clip the satellite images, limiting the analysis to the study area. In this study, the supervised classification technique

was used to produce land use maps of the study area in the years 2014 and 2021. Thus, the maximum likelihood classification algorithm was applied. This algorithm computed the mean of the data after calibrating the normality of data in a class and classified the class of non-classified pixels to a class that has the highest possibility (Asad and Bais 2020). Based on this analysis, the land use maps of the study area were divided into five classes, i.e., water, bare area, urban, rural, and forest (Fig. 2). This land use classification was very useful to determine the boundary of each land use. Then, we could identify precisely the UHI intensity value in each land use. An analysis of accuracy was conducted by equalizing the estimated land uses with a reference land use map. To analyze the land surface temperature (LST) over the Hulu Langat region during the study period, we used time series Landsat 8 TIRS images using band 10. A specific equation (Eq. 1) has been applied to obtain the LST (Stathopoulou and Cartalis 2007). This approach has been widely used in many studies (Avdan and Jovanovska 2016).

$$LST = \left(\frac{BT}{1 + 1(w \times \frac{BT}{p} \times \ln e)} \right) - 273.15 \quad (1)$$

BT is at sensor brightness temperature, W is the emitted radiance wavelength, e is emissivity, and p is 1.438×10^{-2} m K. The LST layers in 2014, 2016, 2018, and 2021 were then used for further analysis of UHI intensity over the study area.

Accuracy assessment

Land use classification

Accuracy analysis was carried out to know the closeness of the predicted values with the true values in real conditions. To analyze the accuracy of the land use map, the confusion matrix was produced (Table 2). The table indicates values for the overall accuracy, user's accuracy, producer's accuracy, and also the Kappa coefficient value. A total of 100 sample points were chosen from Google Earth and compared to the predicted land use map. The overall accuracy represents if all reference points were well-mapped and classified. The overall accuracy was computed by Eq. 2 (Choudhury et al. 2019).

$$\text{Overall accuracy} = \frac{\sum \text{Diagonal value}}{N} \times 100 \quad (2)$$

Then, the accuracy of each land use category was calculated by the user's accuracy and producer's accuracy analyses. The user's accuracy was determined by dividing the matched total of points for each land use category by

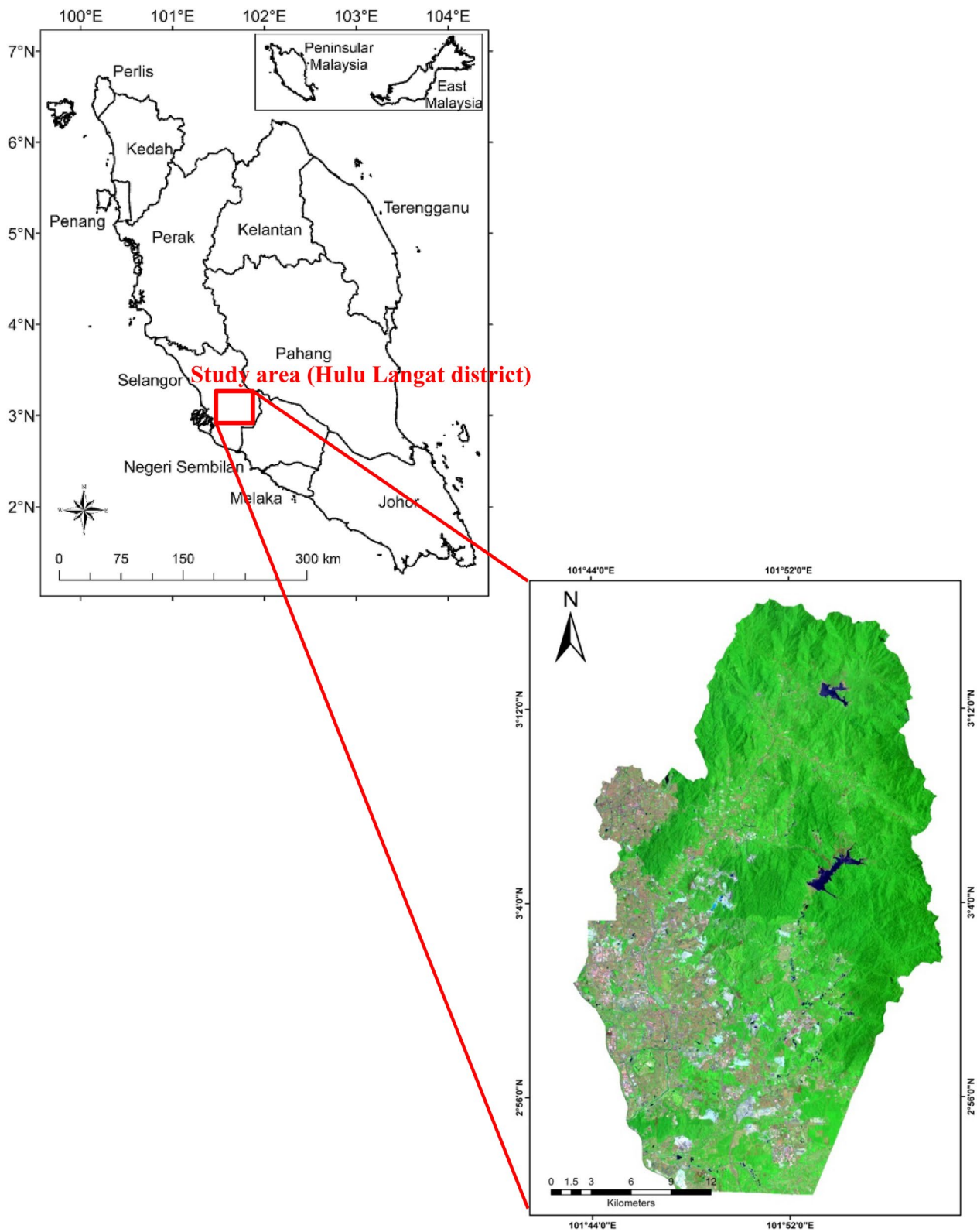


Fig. 1 Location of Hulu Langat district in the southwestern of Peninsular Malaysia. A Landsat 8 image with natural color composite (RGB: 753) is applied to present the district's border

Table 1 Specification of satellite data used in this study

Date of acquisition	Satellite	Sensor	Source
10 July, 2021	Landsat 8	OLI/TIRS	USGS Earth Explorer
18 July, 2018	Landsat 8	OLI/TIRS	USGS Earth Explorer
12 July, 2016	Landsat 8	OLI/TIRS	USGS Earth Explorer
14 July, 2014	Landsat 8	OLI/TIRS	USGS Earth Explorer

the total of points in the similar category and redoubling that value with 100. The user’s accuracy was computed using Eq. 3.

$$\text{User's accuracy(\%)} = \frac{\Sigma \text{ Diagonal value of row}}{\text{Row total}} \times 100 \tag{3}$$

The producer’s accuracy showed the effectiveness of the analysis was done. It was determined by dividing the total of matched points by the total of points from the reference data set and redoubling that value with 100. The producer’s accuracy was determined using Eq. 4 (Choudhury et al. 2019).

$$\text{Producer's accuracy(\%)} = \frac{\Sigma \text{ Diagonal value of column}}{\text{Column total}} \times 100 \tag{4}$$

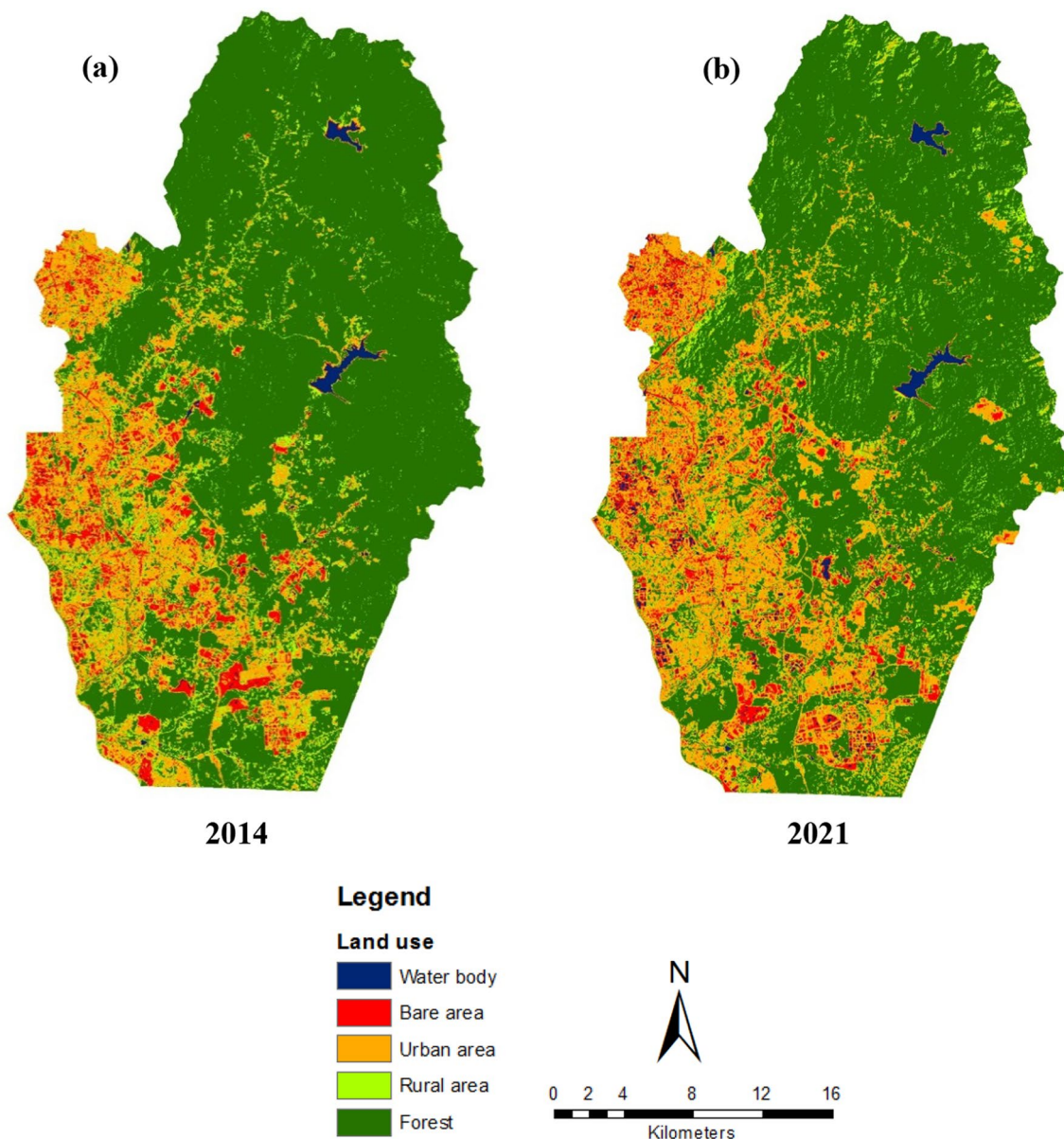


Fig. 2 Land use maps obtained from the Landsat 8 satellite images over the study area in **a** 2014 and **b** in 2021. Land use category in the study area consisted of five classes, including water body, bare area, urban area, rural area, and forest

Table 2 Confusion matrix of the land use classification using supervised classification

Land cover class	Bare land	Rural	Waterbody	Urban	Forest	Row total	User's accuracy (%)
Bare land	0	0	0	0	3	3	100
Rural	3	0	0	12	0	15	80
Waterbody	0	1	7	0	0	8	88
Urban	0	19	2	0	0	21	90
Forest	24	0	0	1	0	25	95
Column total	27	20	9	13	3	72	Overall accuracy 90%
Producer's accuracy (%)	89	95	78	92	100		

Table 3 Overall accuracy and Kappa statistic using supervised classification method

Method	Overall accuracy (%)	Kappa accuracy (%)	Kappa coefficient
Supervised classification	90	87	0.87

The Kappa coefficient (*K*) was one of the multivariate methods for determining accuracy as matched to a random value. The coefficient number differed from - 1 to 1. A negative value showed the performance of the classification was bad, while a 0 value showed the process was not good. The value was near 1 showed the process carried out was good (Rwanga and Ndambuki 2017). The Kappa coefficient was computed using Eq. 5 and the result is shown in Table 3.

$$K = \frac{N \sum_{i=1}^r x_{ii} - \sum_{i=1}^r (x_i + Xx_{+1})}{N^2 - \sum_{i=1}^r (x_{ii}Xx_{+1})} \tag{5}$$

where *r* was the total of row and column in error matrix, *N* was the total of observation (pixels), *x_{ii}* was observation in row *i* and column *i*, *x_{i+}* was slight total of row *i*, *x_{+i}* was slight total of column *i*.

LST validation

In this study, we compared near-surface air temperature data from meteorological stations with our predicted LST value (Table 4). This method has been widely used by many researchers to validate LST in their studies (White-Newsome et al. 2013; Li et al. 2013). Real-time

surface air temperature data sets were acquired from the National Oceanic and Atmospheric Administration open portal for meteorological stations in the study area.

UHI intensity analysis

The LST of the Hulu Langat region was derived from the Landsat 8 TIRS data over distinct time periods. The thermal infrared sensor (TIRS) could be used to quantify LST by utilizing a new thermal band technology that used quantum physics to sense heat. This approach was considered better than an older approach using the MODIS sensor. To diminish cloud disturbances, we selected the minimum percentage of cloud cover over the study area (<10%). Then, LSTs in Hulu Langat region were obtained from satellite images through the extraction tool in ArcGIS. We overlaid the land use maps of the study area, so that the mean LST for every land use could be identified and the urban heat island level could be assessed by a ratio of LST in urban areas and their surrounding areas.

In this study, we adopted the perspective of UHI from Zhang et al. (2023) who used the average LST in rural area to indicate the average LST in the entire study area. This was carried out to assess the variation of temperature between urban and rural lands. Coupled with a land use map, the mean LST for each land use category could be determined, also the UHI intensity could be represented by the LST variation between urban and peripheral areas. Furthermore, the UHI intensity could be grouped into five primary classes, as shown in Table 5. The UHI intensity index could be determined as specified below (Huang et al. 2019).

Table 4 Details and difference between LST and air temperature in the study area

Station	Station ID	2014			2016			2018			2021		
		LST	Air temperature	Difference	LST	Air temperature	Difference	LST	Air temperature	Difference	LST	Air temperature	Difference
Kuala Lumpur International	MYM00048650	33.5	33.0	0.5	35.5	34.0	1.5	27.0	27.9	0.9	28.0	28.8	0.8

Table 5 UHI intensity index

UHI (°C)	Degree	Note
< 0	Very low	Location with extremely low temperatures, demonstrating that there is no difference in LST between urban and rural areas
0–0.1	Low	Low temperature region, suggesting there is little difference in LST between urban and rural areas
0.1–0.2	Medium	Area with a moderate temperature, indicating a moderate LST variation between urban and rural areas
0.2–0.3	High	High temperature zone reflecting a significant LST gap between urban and rural locations
> 0.3	Very high	Extremely high temperatures, which show that there is a significant LST variation between urban and rural regions

$$\text{UHI} = (T_i - T_s) / T_s \quad (6)$$

The UHI intensity index, stated in LST variation in a region. T_i is the LST of the i th pixel, and T_s is the average LST in rural areas.

The land contribution index analysis

The effects of land use were investigated to obtain a comprehensive analysis of the association between land use and its effect on UHI intensity. To assess the impact of different land uses on the UHI, 839 randomly selected points were placed throughout the study area. Then, all points were applied to extract their corresponding LST value for 2014–2021. The time-series thermal effect of every land use over the Hulu Langat region could be calculated using the LCI equation below (Huang et al. 2019).

$$\text{LCI} = (T_i - M) \times P_i \quad (7)$$

T_i is the mean temperatures of the i th land use, i indicates land use type (1–5), P_i represents a ratio of the i th land use to whole study site, M is the mean temperatures in whole study area, and LCI represents a benchmark to calculate a thermal effect of land uses on the urban heat island intensity during the study period. LCI greater than 0 indicates that land use has a positive impact on increasing the urban heat island, while LCI less than 0 indicates that land use has a lessening effect on the urban heat island.

Results and discussion

The spatial variation of UHI effects over the Hulu Langat region

According to the estimated UHI maps (Fig. 3), areas of UHI over the Hulu Langat region have extended from the 2014 to 2021 periods. There was a gradual increase in each year of study. The impact of UHI covered almost half of the entire region with various intensities, except for the northern and eastern parts of the region that had a high forest density (Fig. 3). This result was consistent with the stack profile of land surface temperature in the study area (Fig. 4), which was extracted from the central to the peripheral areas. The LST profile showed a

decreasing trend, which was associated with the locations of urban areas in the west and forests or green spaces in the east. This result was in line with a study in China which found the LST indicated an increasing pattern and was more concentrated in the central zone (urban area), while low temperature tended to concentrate in the borderland (Guo et al. 2020). In 2014, the impact of UHI on the study area was found to be weak, with 136.26 ha of areas under high UHI conditions and 0.09 ha at very high UHI. As compared with 2016, the UHI effect significantly increased around 321.66 ha and 1.44 ha of areas with high and very high UHI levels, respectively. This condition also showed a gradual increase in the following years, 2018 and 2021. Bala et al. (2021) also found the same result that the UHI intensity in Varanasi city of India rose from 0.36 in 1989 to 0.87 in 2018. According to the World Bank Group official report in 2021, the annual maximum daily temperature in Malaysia was around 33 °C, and based on the RCP8.5 projection, mean daily maximum temperatures would exceed 33 °C by the end of the century. The impact of UHI in the Hulu Langat region indicated a continuously increasing trend. This was in line with the rapid urbanization of the study area since this decade. Based on another study by Grigoraş and Urişescu (2019), the construction works affected hard surfaces and then converted them to latent heat fluxes.

A great UHI impact was recorded in 2021 with a total area of 1489.59 ha and 25.74 ha for high–very high UHI levels, indicating the study area was sustaining a severe UHI effect. The UHI zones were primarily spread from the southern to western parts of the study area. As the intensity increased, these main areas gradually emitted radiation to the peripheral areas. Areas with experiencing low to high UHI effects could be assessed using the land use map (Fig. 2). Very low temperatures and UHI effects were constantly found in forests. The UHI effect on water bodies was also lower than other land use types, indicating forest and water bodies potentially eased the UHI effect. A study by Wang et al. (2020) found the UHI intensity attributed from the water bodies in Wuhan, China was greatly associated with the local LST. The distribution of water bodies had a prominent task in

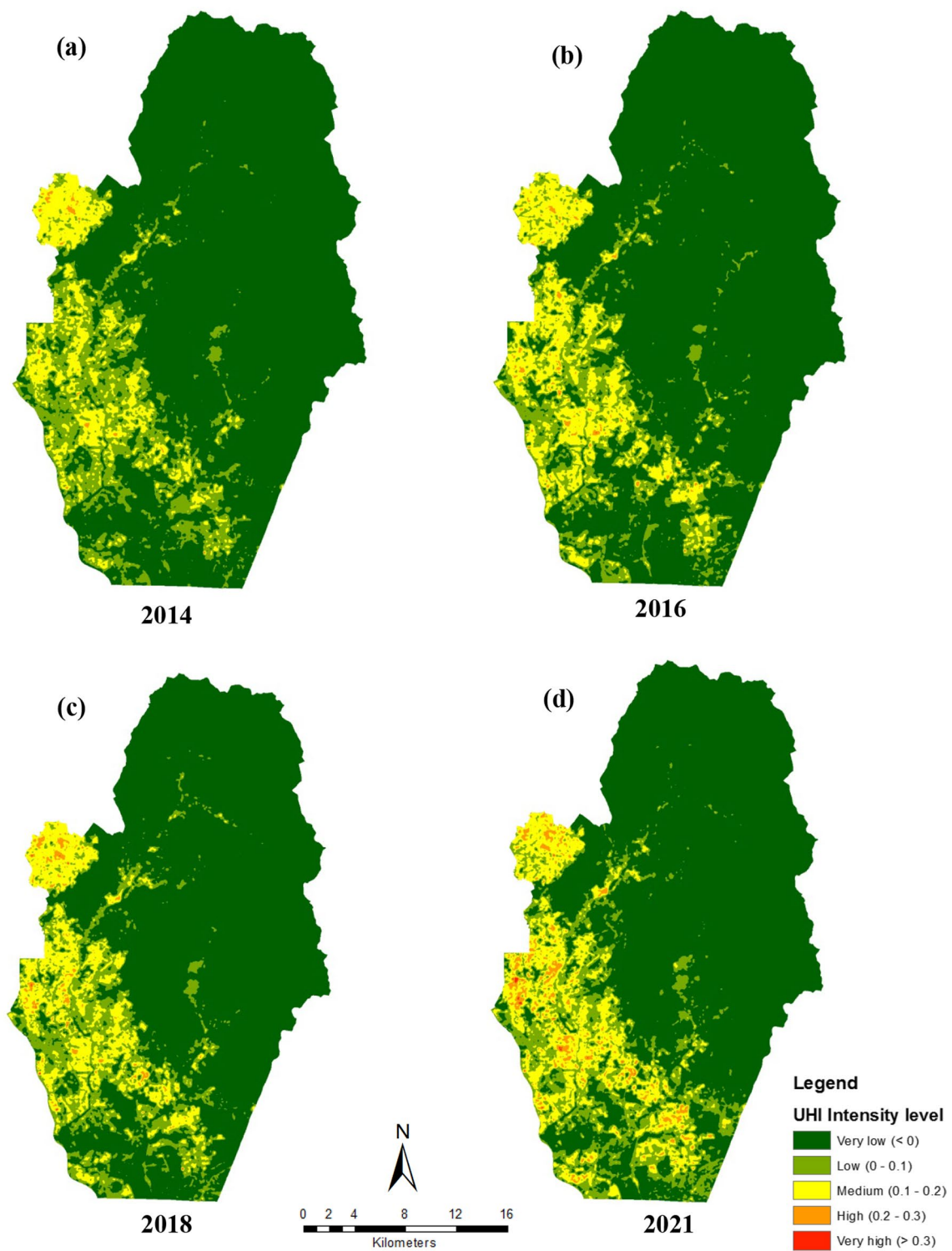


Fig. 3 Spatial variation of UHI over the study area across the study period; **a** 2014, **b** 2016, **c** 2018, and **d** 2021. The UHI intensity of the study area ranged from very low to very high level

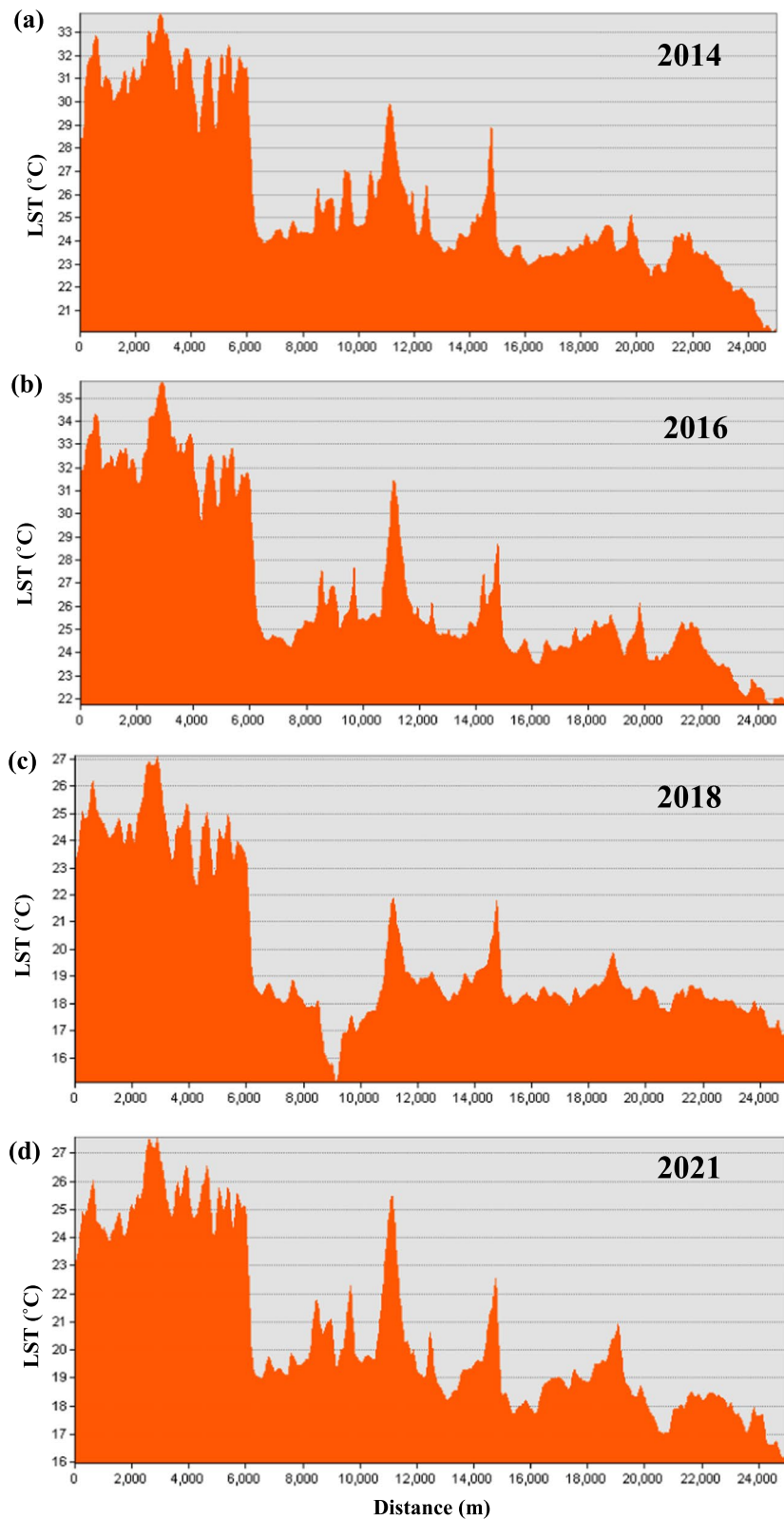


Fig. 4 Stack profile of the land surface temperature (LST) across the study area (from the western to eastern sides of the study area). The LST profiles tend higher in the west and lower toward east part

diminishing LST and urban heat islands. The other studies revealed the UHI was closely related to a reduction of green areas in the city (Wang et al. 2022). The lack of green areas would contribute to an increase in heat fluxes and UHI (Lai et al. 2019).

The UHI value showed a gradual increase from 2014 to 2021. The growth of UHI zones was primarily concentrated on the western and southern sides of the study area, which was in line with the urbanization pattern of the Hulu Langat district. The land use map for 2021 showed a decrease in rural areas as compared with 2014, indicating many rural areas have been converted into urban areas. In general, the central area was the heart of the town, consisting of entertainment places, but urbanization in Hulu Langat derived from the western areas and spread the expansion to peripheral areas. This was due to the fact that the Hulu Langat district was located to the west of the capital city, and other larger cities were located to the south of the Hulu Langat district. Urbanization tended to spread westward. The increment of UHI areas from 136.26 ha to 1489.59 ha during the period 2014–2021 (Table 6) indicates that land use types in the study area have undergone significant changes during this decade. Contrarily, the total area of very low UHI areas decreased gradually across the study period (Table 6). This study assumed that the intensive urbanization in the study area not only led to land use changes, but also influenced the UHI effect. Since 2014, the urbanization pattern slowly moved from dense areas to peripherals within the Hulu Langat region, thus the growth of the UHI effect was only focused on urban peripheral areas. This notion was supported by the increased UHI intensity level that started in 2014.

Forest, urban and rural areas were the predominant land uses within the Hulu Langat region (Table 7). Furthermore, urban areas rose from 13,886.1 ha to 18,269.82 ha (31.5% increase) during 2014–2021, which was in line with urbanization activities during that period. On the other hand, there was a slight change in the water body area. The wet season of the Hulu Langat region occurred from November to March which led to a notable increase in water volume in the region. During

Table 6 Classification of each UHI level and its total area (ha) within the study area during 2014–2021

Period	UHI intensity level corresponding to total area (ha)				
	Very low	Low	Medium	High	Very high
2014	64,856.07	12,867.57	6306.93	136.26	0.09
2016	63,841.68	11,342.43	8659.71	321.66	1.44
2018	62,609.76	12,145.23	8816.94	587.88	7.11
2021	59,163.30	13,159.08	10,329.21	1489.59	25.74

Table 7 Total area of each land use within the study area in 2014 and 2021

Land use	2014 (ha)	2021 (ha)
Water body	665.82	1278.72
Bare area	4631.67	4797.45
Urban area	13,886.10	18,269.82
Rural area	7076.43	6866.46
Forest	57,906.90	52,954.47

this season, the region received heavy rains, which frequently caused a big flood. Thus, the total area of the water body in 2021 (1278.72 ha) was much higher than in 2014 (665.82 ha). In addition, the declines in forest and rural areas, together with the expansion of urban areas, including construction activities, were considered as main contributors to the UHI effect in recent years.

The association between UHI and land use type according to LCI

Figure 5 explains that the urban areas indicated the most positive impacts on the UHI. The urban areas gave the most substantial heat counts to the Hulu Langat region during 2014–2021. Our study showed the same result as a study by Yue et al. (2019) who found a higher UHI located in the higher built-up area as compared to the smaller built-up area in cities of China. Rapid urbanization during the 7 years in our study area has made 31.5% of urban areas expand in 2021, contributing to a greater impact on the UHI. Contrarily, forest and water bodies assisted in diminishing the UHI effect. Furthermore, the forest area gave the most accent to the UHI effect as compared with other land use types. The maximal value of LCI of a water body ranged from – 0.03 to – 0.01 during 2014–2021 (Fig. 5), indicating temperature values of the water body greatly varied due to fluctuating heat. Similarly, green areas such as forests had an inverse effect on the UHI. The LCI of forest area across the study period varied from – 0.04 to – 0.01 (Fig. 5), which might be due to the reduction in the percentage area of forest. The lower LCI value of the forest in 2021 indicated that the forest area had less capability of alleviating the UHI effect. Green areas in urban environments had the ability to absorb toxic pollutants, cleaning the air and ecosystems. Furthermore, it could enhance the microclimate to equilibrate environmental issues due to urbanization and development activities (Zellweger et al. 2020). A study by Pramanik and Punia (2020) in India found that the UHI was lower in the districts of south and southwest Delhi due to less built-up area and the higher existing of greenery spaces.

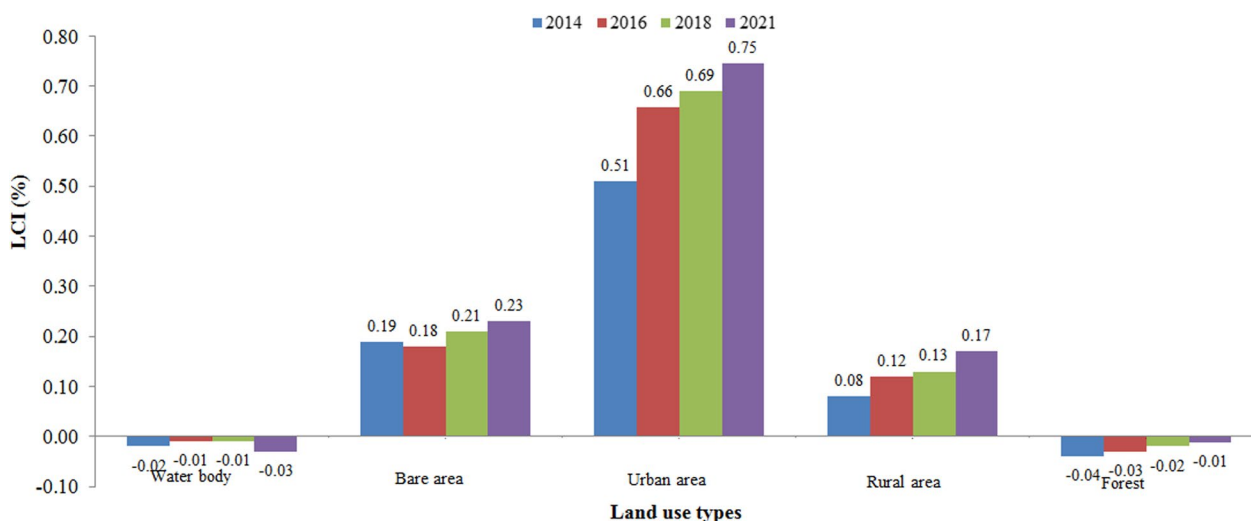


Fig. 5 Land contribution index (LCI) of each land use from 2014 to 2021 in the study area. Urban land use area was considered as the highest impact on the urban heat intensity within the study area

Distinct land use types indicated various levels of impact on the UHI across time. For instance, the urban area revealed the highest contributor to heat across the study period (0.51–0.75). Based on time series analysis, we assumed that the high contributors of almost all land use to the UHI effect occurred in 2021, but in 2014, we found rural areas showed a higher contribution of heat than in 2021. We believed activities in urban areas, where there was construction and development work, such as the building of infrastructure, residential units, and facilities for new municipal areas, have retained LCI to a high level. Despite the fact that the average LST value in 2021 was slightly lower than in previous years, the total percentage area of high temperature increased over time. This result was consistent with a study by Yang et al. (2016), which reported that the construction area had the highest contribution in their study. In the tropical region, rainfall patterns had a notable effect on the contribution of fluctuating LCI values, and the increasing of urban green areas would assist in dropping the amount of heat from the urban area. Meanwhile, in the subtropical region, the spring and summer seasons resulted in more urban green spaces, which led to more heat dissipation. In dry conditions, the reduction of urban green areas directly decreased the urban areas’ ability to absorb heat (Pramanik and Punia 2020).

Many UHI studies agreed that urbanization was a major driver of rising land surface temperatures and exacerbating UHI effect. In contrast, a forest or green area and a water body had an inverse influence on the UHI effect. A study by Tan and Li (2013) reported that green area coverage influenced the UHI intensity in

Beijing, China, with the LST value of green areas being lower than other residential and commercial areas. Another study by Morakinyo et al. (2016) found tree planting was closely associated with a decrease in temperature in a typical indoor setting compared with bare land. Very low UHI intensity was recorded at the forest land and water body, and it was almost constant during the study period. Because of the high amount of heat capacity, the temperature distribution on the water body varied little on this occasion. In similar conditions, very high UHI values were constantly spread throughout urban areas. The flow of urban expansion from the west to the central parts of the study area could be seen from the land use maps. This corresponded to the expansion of urbanization in Hulu Langat, which spread to the peripheral areas in the following years.

In addition, the medium UHI intensity started to experience a substantial change from the western to the southern areas in 2016. Low UHI intensity was more located in the northern and eastern parts. There was a great conversion of forest area in the southern part, which corresponded to an increase in UHI intensity around that area. On the UHI intensity map, we could see the changes in moderate UHI intensity over the study area. From 2014 to 2018, the medium UHI intensity was concentrated in rural and agricultural areas, and subsequently, it migrated to urban areas after 7 years. For further details, we could see that the strong UHI is located in the Hulu Langat district in Fig. 6. The very high UHI values were mostly observed in the western corner part of the region, which was categorized into urban and bare areas. There was an increase in

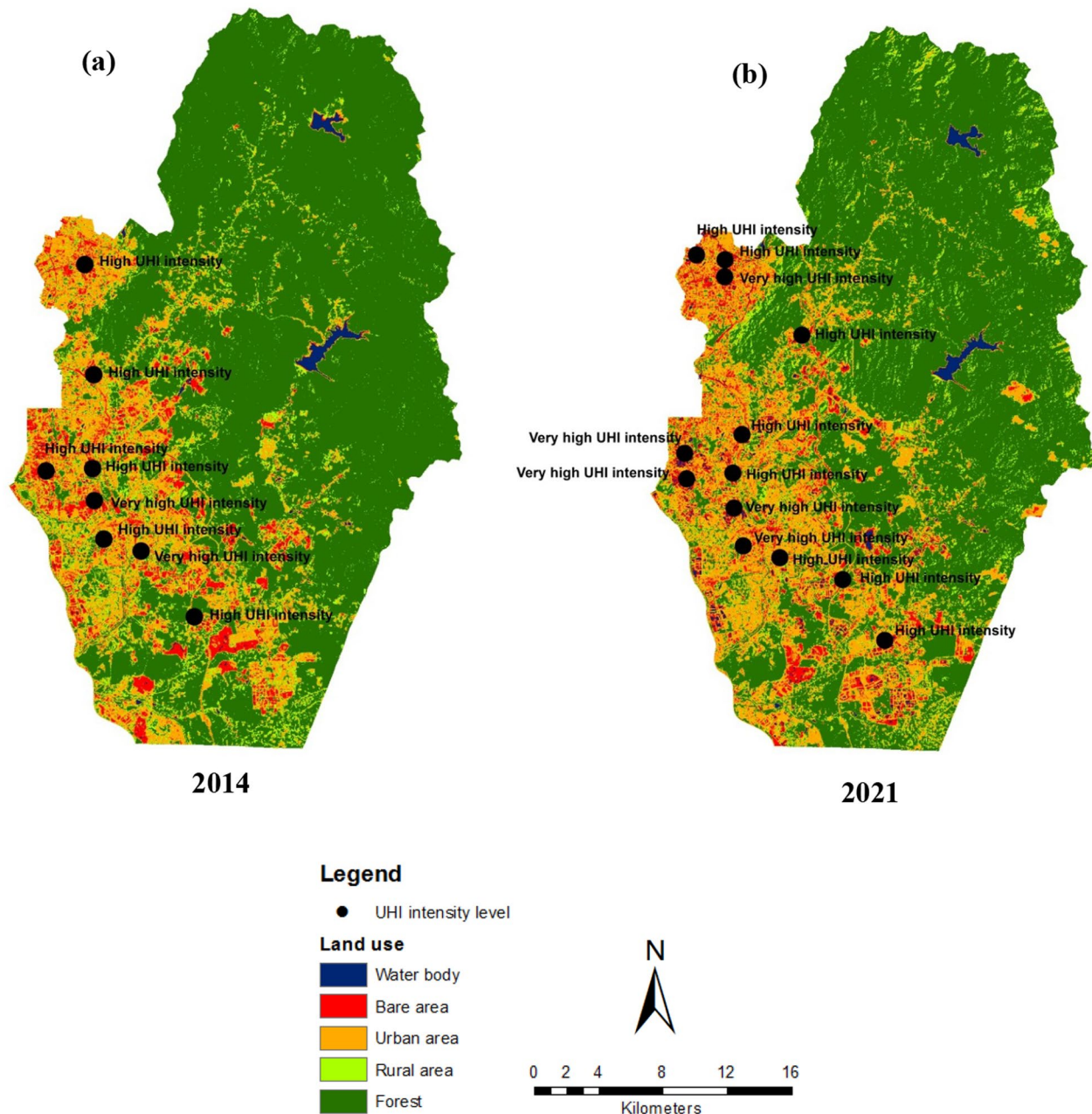


Fig. 6 Very high and high UHI intensity levels located in land use map of the period; **a** 2014 and **b** 2021. Very high and high UHI intensity levels was mostly found in urban and bare areas

very high UHI hotspots from 2014 to 2021. As a whole, we realized there was a limitation in our study, because all analyses were based on the interpretation of remote sensing and GIS techniques. Therefore, for future studies, we suggest using other satellite data with higher spatial and temporal resolution to diminish the effect of atmospheric disturbances. In addition, it was also needed to deeply investigate the impact of anthropogenic activities, social and economic aspects, and other drivers of the UHI effect.

Conclusions

In this study, we successfully used UHII and land contribution indexes for analyzing UHI intensity and its association with land use types in the Hulu Langat district of Malaysia. The high UHI intensity areas had significantly expanded during 2014–2021. These high UHI intensity areas were mainly concentrated in the western and southern parts of the study area. The urban areas were found as the greatest contributors to UHI effect during the

study period, whereas forests and water bodies showed the smallest contributors to the UHI effect. The UHI intensity in urban areas was consistent with the increasing total area of urban lands. In contrast, the increase in urban green areas would assist in reducing heat capacity, also UHI effect over the study area at once. Our results can help in arranging an effective way for future land resource management policy in the Hulu Langat district of Malaysia.

Author contributions

Conceptualization and supervision: MR; writing review and editing: MR, WMRI, SAR and HGA; data curation and formal analysis: MR, WMRI and SAR; evidence collection, review, and editing: SD, SN, HGA, HA, AAA and MM.

Funding

This project was funded by Princess Nourah bint Abdulrahman University Research Supporting Project Number PNUURSP2022R241, Princess Nourah bint Abdulrahman University, Riyadh, Saudi Arabia.

Availability of data and materials

The data sets used and/or analyzed during the current study are available from the corresponding author on reasonable request.

Declarations

Ethics approval and consent to participate

Not applicable.

Consent for publication

Not applicable.

Competing interests

On behalf of all authors, the corresponding author states that they have no known competing financial interests or personal relationships that could have appeared to influence the work reported in this paper.

Author details

¹Department of Chemical Engineering, Faculty of Engineering, Universitas Sriwijaya, Indralaya 30662, South Sumatra, Indonesia. ²Department of Earth Sciences and Environment, Faculty of Science and Technology, Universiti Kebangsaan Malaysia, 43600 Bangi, Selangor, Malaysia. ³Department of Environmental Science, Faculty of Science and Natural Resources, Universiti Malaysia Sabah, 88400 Kota Kinabalu, Sabah, Malaysia. ⁴Geography Department, Faculty of Arts and Humanities, Tartous University, Tartous, Syria. ⁵Department of Geography, College of Arabic Language and Social Studies, Qassim University, Buraydah 51452, Saudi Arabia. ⁶Department of Geography, College of Arts, Princess Nourah Bint Abdulrahman University, Riyadh 11671, Saudi Arabia.

Received: 9 January 2023 Accepted: 10 July 2023

Published online: 18 July 2023

References

- AlDousari AE, Kafy AA, Saha M, Fattah MA, Almulhim AI, Al Rakib A et al (2022) Modelling the impacts of land use/land cover changing pattern on urban thermal characteristics in Kuwait. *Sustain Cities Soc* 86:104107
- AlDousari AE, Kafy AA, Saha M, Fattah MA, Bakshi A, Rahaman ZA (2023) Summertime microscale assessment and prediction of urban thermal comfort zone using remote-sensing techniques for Kuwait. *Earth Syst Environ* 7:435
- Asad MH, Bais A (2020) Weed detection in canola fields using maximum likelihood classification and deep convolutional neural network. *Inf Proc Agric* 7(4):535–545
- Avdan U, Jovanovska G (2016) Algorithm for automated mapping of land surface temperature using LANDSAT 8 satellite data. *J Sens* 2016:1480307
- Bala R, Prasad R, Yadav VP (2021) Quantification of urban heat intensity with land use/land cover changes using Landsat satellite data over urban landscapes. *Theoret Appl Climatol* 145:1–12
- Cai D, Fraedrich K, Guan Y, Guo S, Zhang C, Zhu X (2019) Urbanization and climate change: insights from eco-hydrological diagnostics. *Sci Total Environ* 647:29–36
- Cheela VS, John M, Biswas W, Sarker P (2021) Combating urban heat island effect—a review of reflective pavements and tree shading strategies. *Buildings* 11(3):93
- Choudhury D, Das K, Das A (2019) Assessment of land use land cover changes and its impact on variations of land surface temperature in Asansol-Durgapur Development Region. *Egypt J Remote Sens Space Sci* 22(2):203–218
- Correia Filho WLF, de Oliveira-Júnior JF, Santiago DDB, Abdo HG, Almo-hamad H, Al Dughairi AA, da Silva Junior CA (2023) The assessment of climatic, environmental, and socioeconomic aspects of the Brazilian Cerrado. *Ecol Process* 12:19
- Deng F, Yang Y, Zhao E, Xu N, Li Z, Zheng P et al (2022) Urban heat island intensity changes in Guangdong-Hong Kong-Macao Greater Bay Area of China Revealed by Downscaling MODIS LST with deep learning. *Int J Environ Res Public Health* 19(24):17001
- Dhar RB, Chakraborty S, Chattopadhyay R, Sikdar PK (2019) Impact of land-use/land-cover change on land surface temperature using satellite data: a case study of Rajarhat Block, North 24-Parganas District, West Bengal. *J Indian Soc Remote Sens* 47(2):331–348
- Elmes A, Healy M, Geron N, Andrews MM, Rogan J, Martin DG et al (2020) Mapping spatiotemporal variability of the urban heat island across an urban gradient in Worcester, Massachusetts using in-situ Thermochrons and Landsat-8 Thermal Infrared Sensor (TIRS) data. *Giscience Remote Sens* 57(7):845–864
- Fabrizi R, Bonafoni S, Biondi R (2010) Satellite and ground-based sensors for the urban heat island analysis in the city of Rome. *Remote Sens* 2(5):1400–1415
- Grigoraş G, Urişescu B (2019) Land use/land cover changes dynamics and their effects on surface urban heat island in Bucharest, Romania. *Int J Appl Earth Obs Geoinf* 80:115–126
- Guo A, Yang J, Xiao X, Xia J, Jin C, Li X (2020) Influences of urban spatial form on urban heat island effects at the community level in China. *Sustain Cities Soc* 53:101972
- Huang Q, Huang J, Yang X, Fang C, Liang Y (2019) Quantifying the seasonal contribution of coupling urban land use types on Urban Heat Island using Land Contribution Index: a case study in Wuhan, China. *Sustain Cities Soc* 44:666–675
- Kafy AA, Rahman MS, Hasan MM, Islam M (2020) Modelling future land use land cover changes and their impacts on land surface temperatures in Rajshahi, Bangladesh. *Remote Sens Appl Soc Environ* 18:100314
- Kafy AA, Rahman MS, Islam M, Al Rakib A, Islam MA, Khan MHH et al (2021) Prediction of seasonal urban thermal field variance index using machine learning algorithms in Cumilla, Bangladesh. *Sustain Cities Soc* 64:102542
- Kafy AA, Saha M, Rahaman ZA, Rahman MT, Liu D, Fattah MA et al (2022) Predicting the impacts of land use/land cover changes on seasonal urban thermal characteristics using machine learning algorithms. *Build Environ* 217:109066
- Karuppasamy MB, Natesan U, Karuppanan S, Chandrasekaran LN, Hussain S, Almohamad H et al (2022) Multivariate urban air quality assessment of indoor and outdoor environments at chennai metropolis in South India. *Atmosphere* 13(10):1627
- Lai D, Liu W, Gan T, Liu K, Chen Q (2019) A review of mitigating strategies to improve the thermal environment and thermal comfort in urban outdoor spaces. *Sci Total Environ* 661:337–353
- Li ZL, Tang BH, Wu H, Ren H, Yan G, Wan Z et al (2013) Satellite-derived land surface temperature: current status and perspectives. *Remote Sens Environ* 131:14–37
- Lyu F, Wang S, Han SY, Catlett C, Wang S (2022) An integrated cyberGIS and machine learning framework for fine-scale prediction of Urban Heat Island using satellite remote sensing and urban sensor network data. *Urban Inf* 1(1):1–15

- Morakinyo TE, Dahanayake KKC, Adegun OB, Balogun AA (2016) Modelling the effect of tree-shading on summer indoor and outdoor thermal condition of two similar buildings in a Nigerian university. *Energy Build* 130:721–732
- Mukherjee F, Singh D (2020) Assessing land use–land cover change and its impact on land surface temperature using LANDSAT data: a comparison of two urban areas in India. *Earth Syst Environ* 4(2):385–407
- Nasir MJ, Ahmad W, Iqbal J, Ahmad B, Abdo HG, Hamdi R, Bateni SM (2022) Effect of the urban land use dynamics on land surface temperature: a case study of kohat city in Pakistan for the period 1998–2018. *Earth Syst Environ* 6(1):237–248
- Nimish G, Bharath HA, Lalitha A (2020) Exploring temperature indices by deriving relationship between land surface temperature and urban landscape. *Remote Sens Appl Soc Environ* 18:100299
- Nurwanda A, Honjo T (2020) The prediction of city expansion and land surface temperature in Bogor City, Indonesia. *Sustain Cities Soc* 52:101772
- Pramanik S, Punia M (2020) Land use/land cover change and surface urban heat island intensity: source–sink landscape-based study in Delhi, India. *Environ Dev Sustain* 22(8):7331–7356
- Rahaman ZA, Kafy AA, Saha M, Rahim AA, Almulhim AI, Rahaman SN et al (2022) Assessing the impacts of vegetation cover loss on surface temperature, urban heat island and carbon emission in Penang city, Malaysia. *Build Environ* 222:109335
- Rendana M, Idris WMR, Rahim SA (2021a) Spatial distribution of COVID-19 cases, epidemic spread rate, spatial pattern, and its correlation with meteorological factors during the first to the second waves. *J Infect Public Health* 14(10):1340–1348
- Rendana M, Idris WMR, Rahim SA (2021b) Atmospheric methane condition over the south sumatera peatland during the COVID-19 pandemic. *Aerosol Air Qual Res* 21(10):210072
- Rendana M, Idris WMR, Abd Rahim S (2022) Effect of COVID-19 movement control order policy on water quality changes in Sungai Langat, Selangor, Malaysia within distinct land use areas. *Sains Malaysiana* 51:1587–1598
- Roy S, Bose A, Majumder S, Roy Chowdhury I, Abdo HG, Almohamad H, Abdullah Al Dughairi A (2022) Evaluating urban environment quality (UEQ) for class-I Indian city: an integrated RS-GIS based exploratory spatial analysis. *Geocarto Int*. <https://doi.org/10.1080/10106049.2022.2153932>
- Rwanga SS, Ndambuki JM (2017) Accuracy assessment of land use/land cover classification using remote sensing and GIS. *Int J Geosci* 8(4):611
- Saha M, Kafy AA, Bakshi A, Almulhim AI, Rahaman ZA, Al Rakib A et al (2022) Modelling microscale impacts assessment of urban expansion on seasonal surface urban heat island intensity using neural network algorithms. *Energy Build* 275:112452
- Shirani-Bidabadi N, Nasrabadi T, Faryadi S, Larjani A, Roodposhti MS (2019) Evaluating the spatial distribution and the intensity of urban heat island using remote sensing, case study of Isfahan city in Iran. *Sustain Cities Soc* 45:686–692
- Stathopoulou M, Cartalis C (2007) Daytime urban heat islands from Landsat ETM+ and Corine land cover data: an application to major cities in Greece. *Sol Energy* 81(3):358–368
- Taiwo BE, Kafy AA, Samuel AA, Rahaman ZA, Ayowole OE, Shahrier M et al (2023) Monitoring and predicting the influences of land use/land cover change on cropland characteristics and drought severity using remote sensing techniques. *Environ Sustain Indicators* 18:100248
- Tan M, Li X (2013) Integrated assessment of the cool island intensity of green spaces in the mega city of Beijing. *Int J Remote Sens* 34(8):3028–3043
- Tepanosyan G, Muradyan V, Hovsepyan A, Pinigin G, Medvedev A, Asmaryan S (2021) Studying spatial-temporal changes and relationship of land cover and surface Urban Heat Island derived through remote sensing in Yerevan, Armenia. *Armenia Build Environ* 187:107390
- Wang W, Liu K, Tang R, Wang S (2019) Remote sensing image-based analysis of the urban heat island effect in Shenzhen, China. *Phys Chem Earth Parts a/b/c* 110:168–175
- Wang L, Hou H, Weng J (2020) Ordinary least squares modelling of urban heat island intensity based on landscape composition and configuration: a comparative study among three megacities along the Yangtze River. *Sustain Cities Soc* 62:102381
- Wang C, Ren Z, Dong Y, Zhang P, Guo Y, Wang W, Bao G (2022) Efficient cooling of cities at global scale using urban green space to mitigate urban heat island effects in different climatic regions. *Urban For Urban Green* 74:127635
- Wei G, Zhang Z, Ouyang X, Shen Y, Jiang S, Liu B, He BJ (2021) Delineating the spatial-temporal variation of air pollution with urbanization in the Belt and Road Initiative area. *Environ Impact Assess Rev* 91:106646
- White-Newsome JL, Brines SJ, Brown DG, Dvonch JT, Gronlund CJ, Zhang K et al (2013) Validating satellite-derived land surface temperature with in situ measurements: a public health perspective. *Environ Health Perspect* 121(8):925–931
- Yang L, Qian F, Song DX, Zheng KJ (2016) Research on urban heat-island effect. *Procedia Eng* 169:11–18
- Yue W, Liu X, Zhou Y, Liu Y (2019) Impacts of urban configuration on urban heat island: an empirical study in China mega-cities. *Sci Total Environ* 671:1036–1046
- Zellweger F, De Frenne P, Lenoir J, Vangansbeke P, Verheyen K, Bernhardt-Römermann M et al (2020) Forest microclimate dynamics drive plant responses to warming. *Science* 368(6492):772–775
- Zhang M, Kafy AA, Xiao P, Han S, Zou S, Saha M et al (2023) Impact of urban expansion on land surface temperature and carbon emissions using machine learning algorithms in Wuhan, China. *Urban Climate* 47:101347
- Zhou X, Xu Z, Liu W, Wu Y, Zhao T, Jiang H et al (2019) Chemical composition of precipitation in Shenzhen, a coastal mega-city in South China: influence of urbanization and anthropogenic activities on acidity and ionic composition. *Sci Total Environ* 662:218–226

Publisher's Note

Springer Nature remains neutral with regard to jurisdictional claims in published maps and institutional affiliations.

Submit your manuscript to a SpringerOpen® journal and benefit from:

- Convenient online submission
- Rigorous peer review
- Open access: articles freely available online
- High visibility within the field
- Retaining the copyright to your article

Submit your next manuscript at ► [springeropen.com](https://www.springeropen.com)